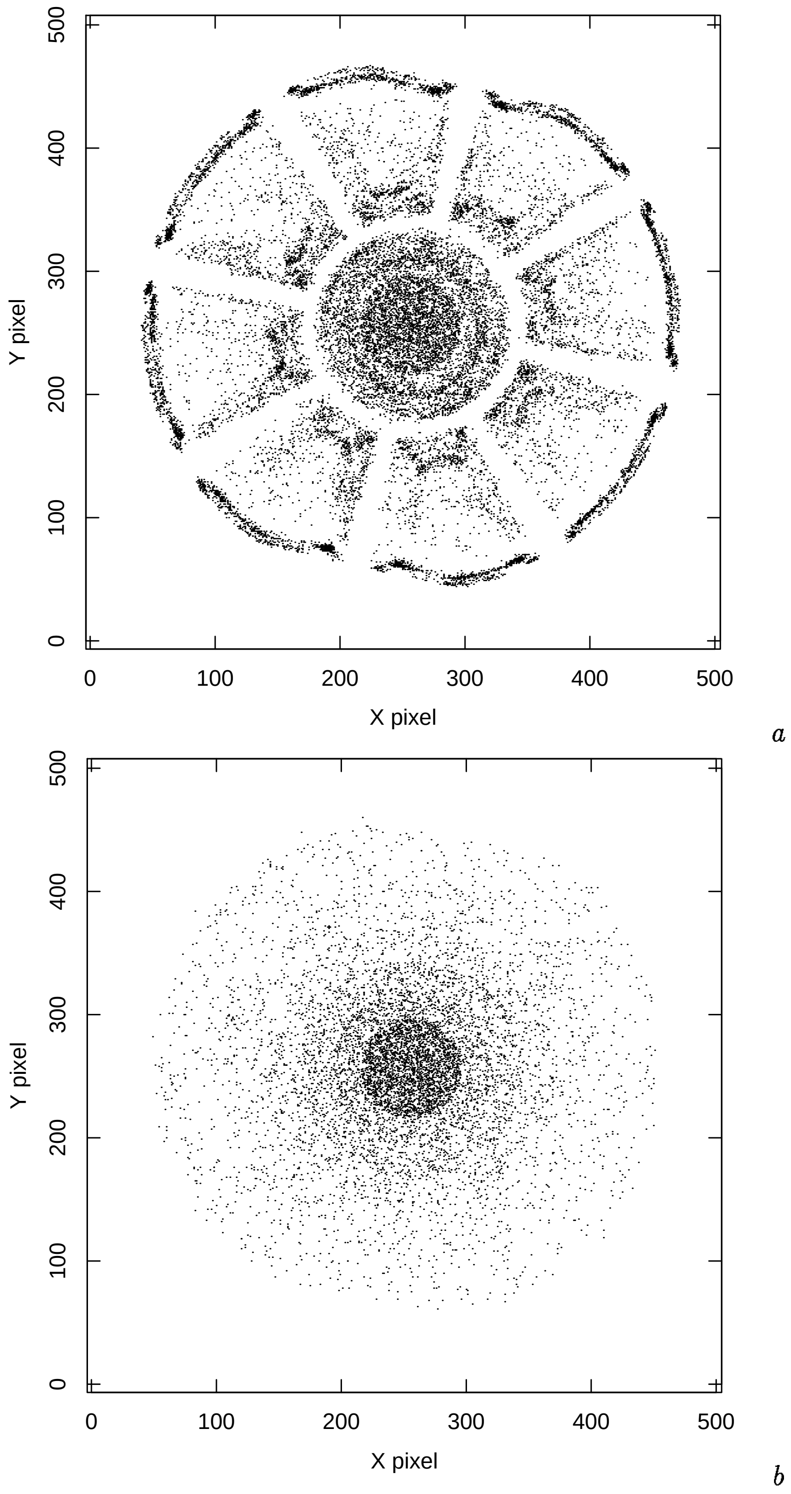

Fig. 1.— Spatial distribution of spurious sources: (*a*) the WT is computed on the photon image; the excess of spurious detections along the ribs and the image edge is evident. (*b*) the WT is computed on the count-rate image; note that no excess of spurious detections is present in this case. The higher density of spurious detections in concentric circular regions towards the image center is expected, and is due to the larger number of "trials" made by the algorithm in the inner part of the image, since it contains more resolution elements and is analyzed at more scales a than the outer regions.

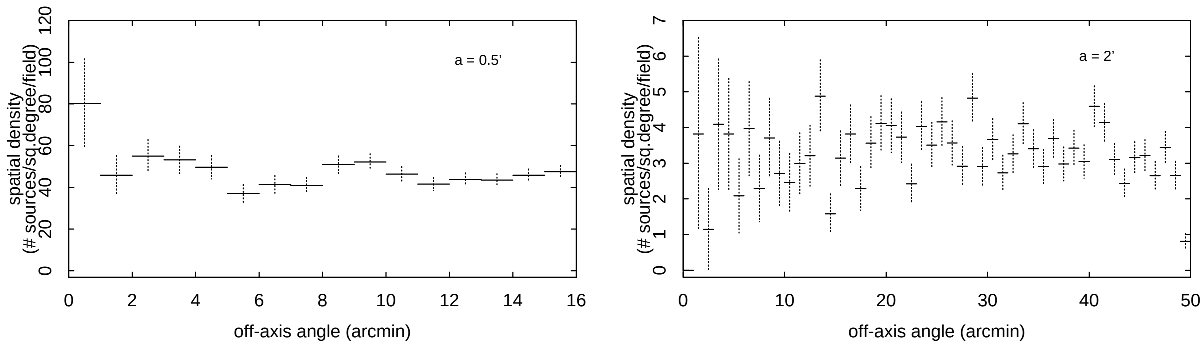

Fig. 2.— Radial distribution of spurious detections (averaged over annuli), for scales $a = 0.5$ arcmin (left panel) and $a = 2$ arcmin (right panel). The error bars are Poisson errors on the total number of detections in each off-axis bin. Both cases are compatible with a uniform distribution. In particular, note that there is no excess of spurious detections at either the position of the circular rib (off-axis ~ 22 arcmin), or along the image edge (~ 50 arcmin).

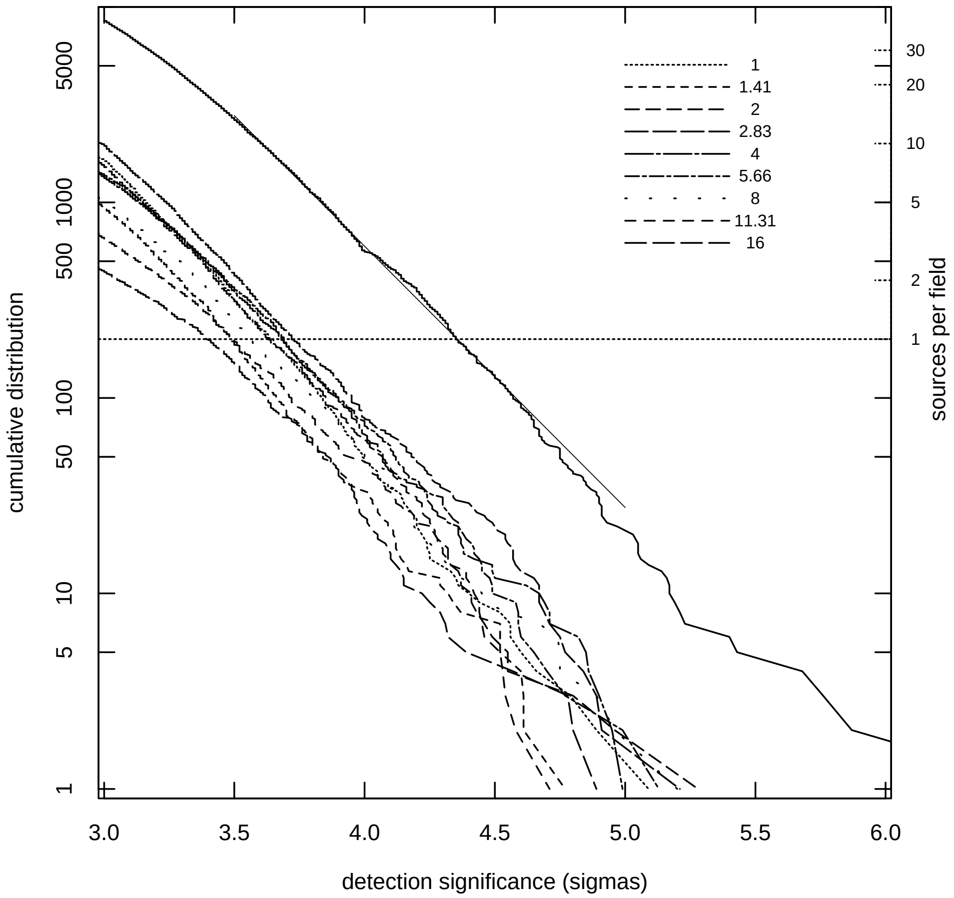

Fig. 3.— Cumulative number of spurious detections vs. significance level $k\sigma$. These distributions are derived from a set of 200 simulations of pure background PSPC fields with exposure time of 10 ksec, and a typical PSPC background of $1.5 \cdot 10^{-3}$ counts/sec arcmin^2 (using the exposure map of the image RP200068). The upper solid thick line refers to the final source list (after cross-identification of detections at different scales a), while the lower distributions refer to detections at various scales separately, as indicated. Also indicated with a thin line segment is the linear fit to the overall distribution for detections in the significance range $3.5 - 5.0\sigma$. The scale on the right side (dotted ticks) indicates the number of spurious detections per image. The horizontal dotted line indicates the level of one spurious detection per simulated field.

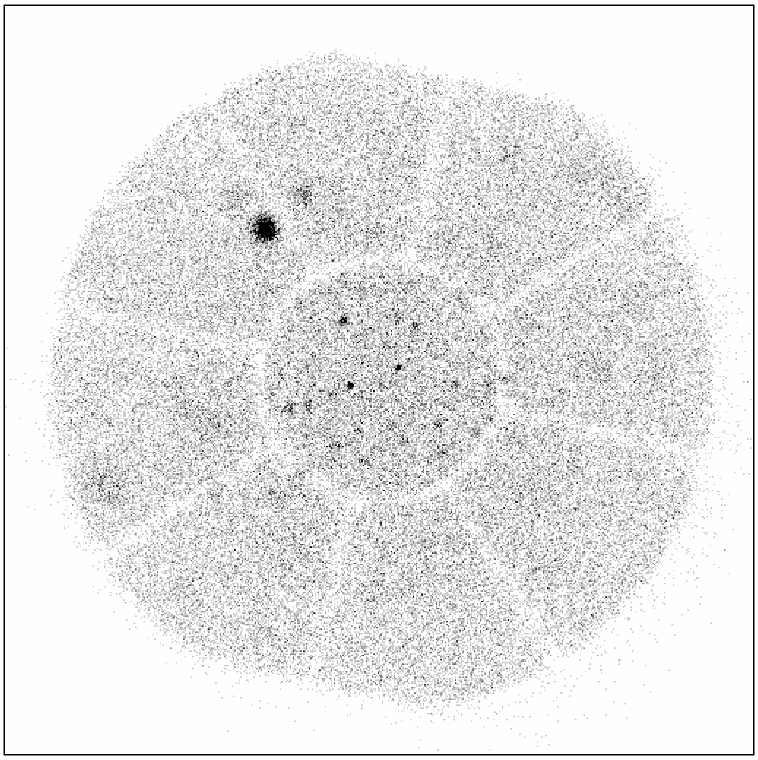

Fig. 4.— Simulated image with point sources. Simulation parameters are as in Figure 3. In this image, 977 simulated sources are present, having a minimum of 5 photons. As is evident, most of these sources only contribute to the background and to its fluctuations.

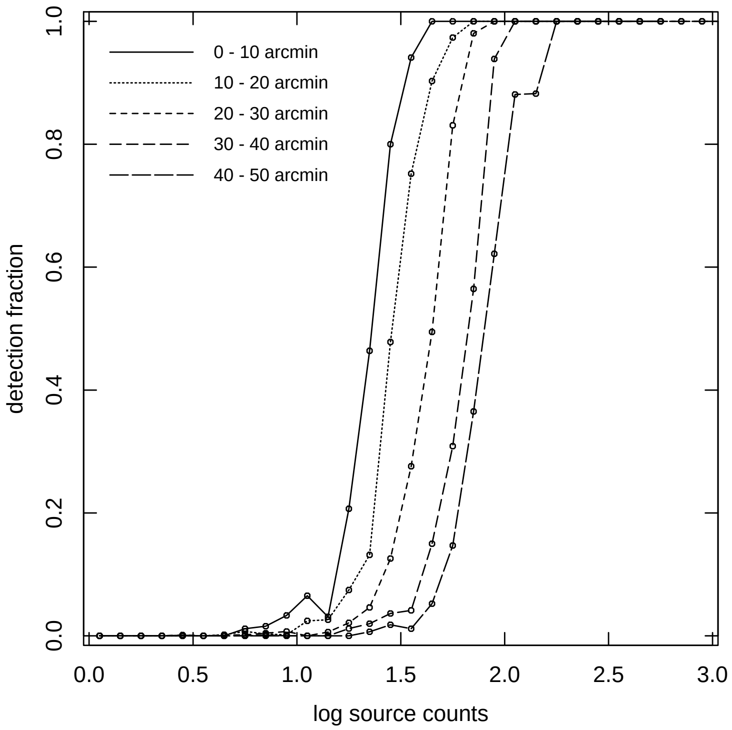

Fig. 5.— Detection efficiency evaluated on simulated data, as a function of source counts and off-axis angle. Simulation parameters are as in Figure 3. The detection threshold is set to 4.2σ, yielding 1.8 spurious sources per field.

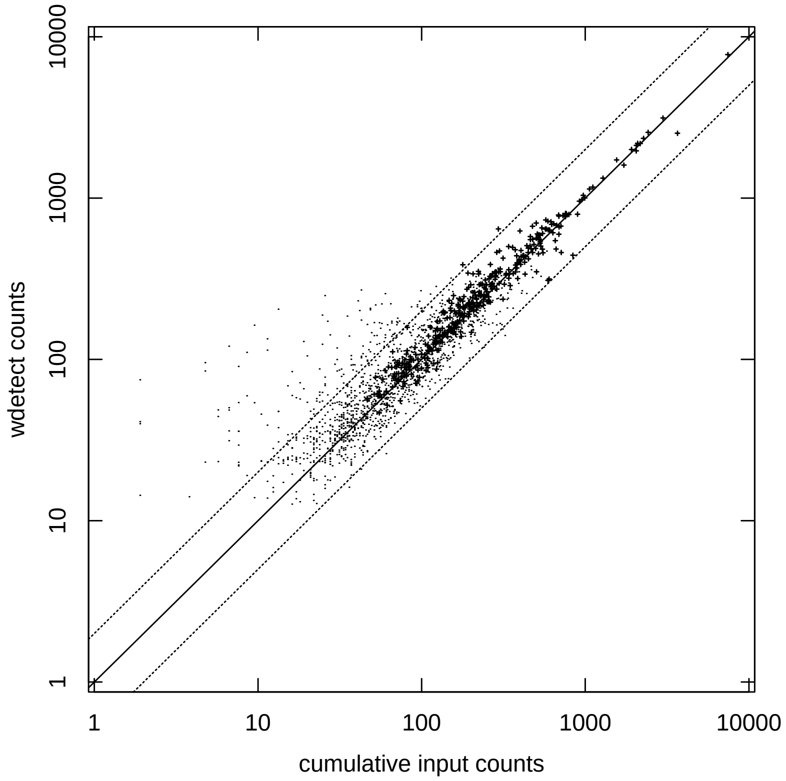

Fig. 6.— Detected vs. input counts. The solid line represents equality, the dotted ones a factor of two difference. Small dots are zeroth-order measurements for weak sources, while crosses are more refined measurements for higher-significance detections, as described in the text.

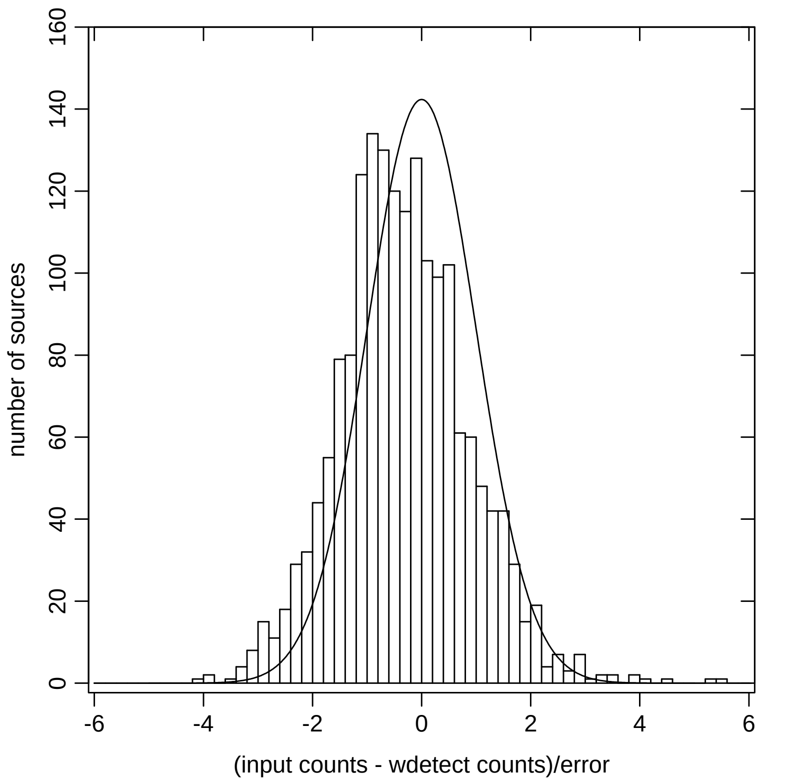

Fig. 7.— Distribution of the difference between input counts and counts estimated by the algorithm, divided by their error. Also plotted in the Figure is a gaussian with zero mean and unit variance.

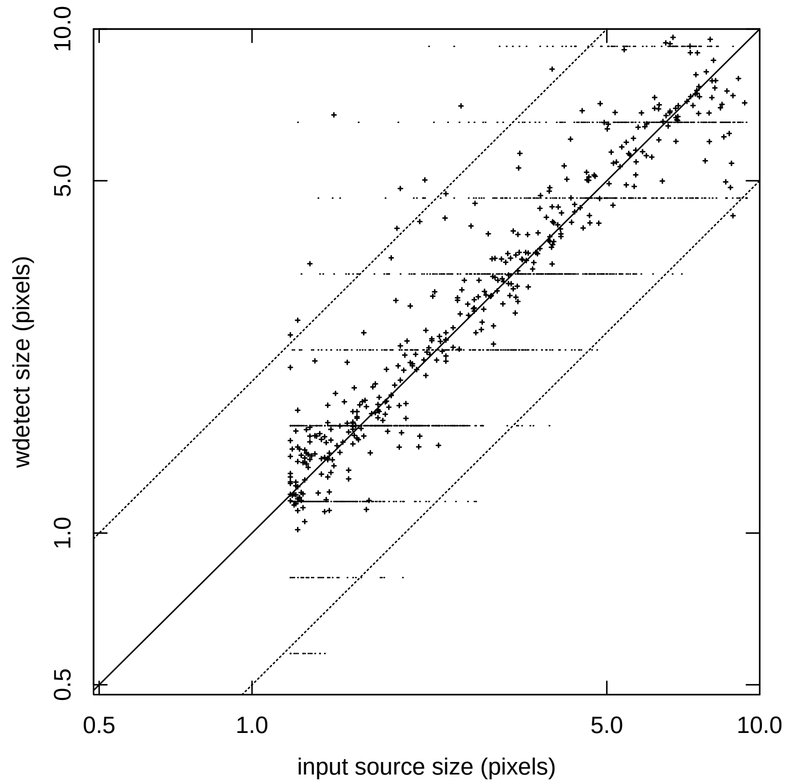

Fig. 8.— Comparison of detected and input sizes. The solid line represents equality, the dotted ones a factor of two difference. Symbols are as in Figure 6.

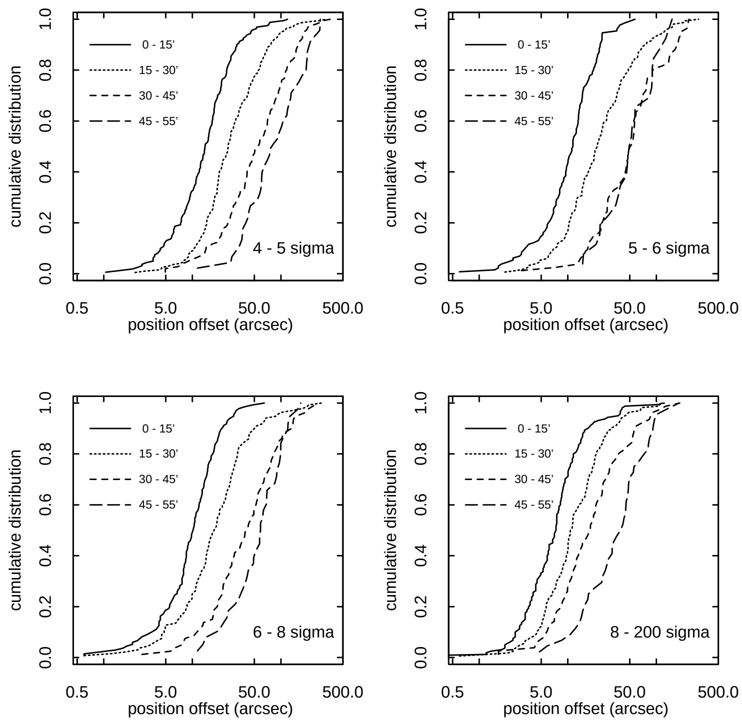

Fig. 9.— Cumulative distributions of positional errors from simulated data, as a function of detection significance and off-axis angle. Note that the cross-identification distance may be as large as a few arcmin even at image center in a very small fraction of cases, since it depends on the detection scale a_{max} and not only on the PSF width σ_{PSF}.

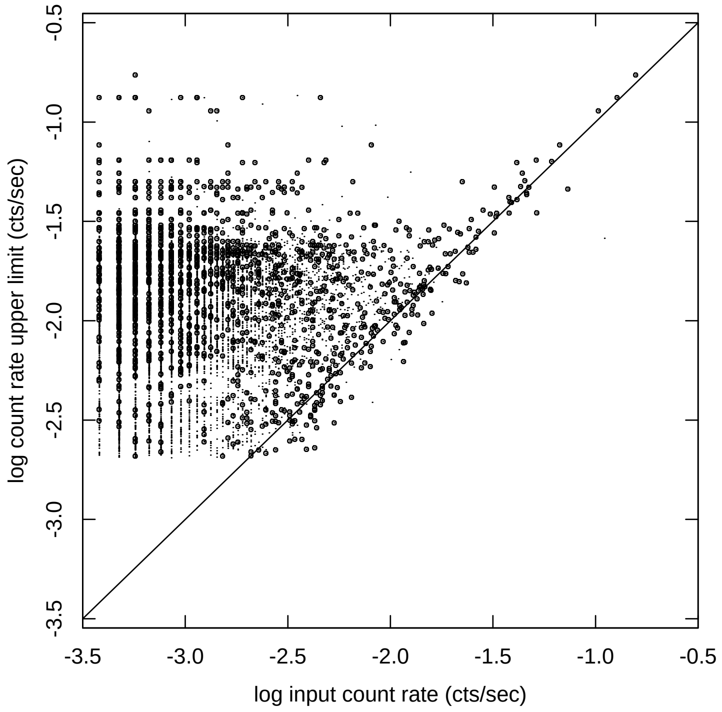

Fig. 10.— Upper limits computed for undetected sources vs. input count rates for simulated sources (small dots). Small circles indicate input sources positionally coincident with detected sources, for which the upper limit has been set equal to the detected count rate. The derived upper limits are consistent with the input values since most of them lie above the equality line, or below it by less than a factor of two.

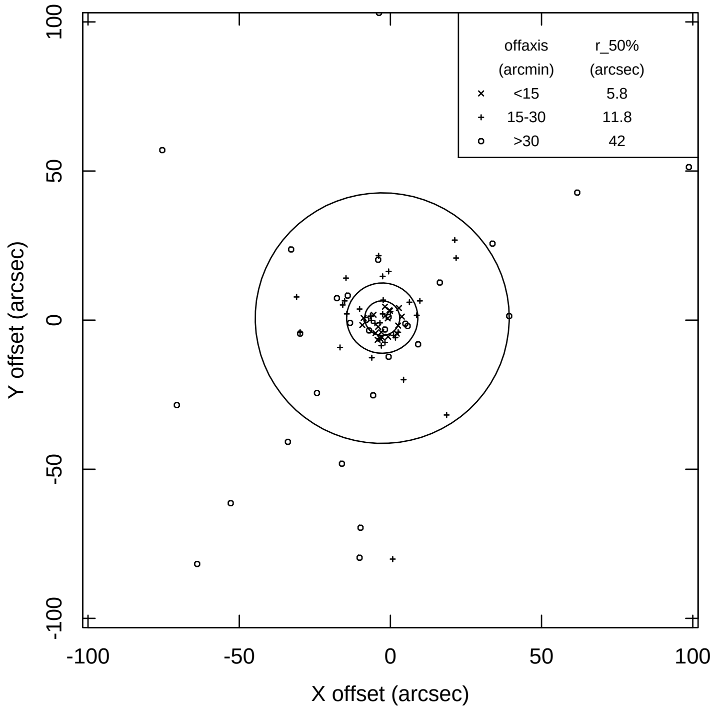

Fig. 11.— Offsets between X-ray and optical positions, for stars in the Pleiades cluster (image RP200068). Different symbols indicate different off-axis ranges: Crosses indicate sources with off-axis less than $15'$, plusses sources between 15-$30'$, and small circles sources beyond $30'$. Large circles indicate the median offset for each off-axis range, and are centered on the median offset for all sources with off-axis $< 30'$.